



# Symmetric double radiative return with $Z \rightarrow q\bar{q}$ final state.

C. Mariotti <sup>1,2</sup>, E. Piotto <sup>1</sup>

## Abstract

The double radiative return events to the  $Z$  where the two emitted photons have similar energy have been studied at LEP with the DELPHI detector at centre-of-mass energies ranging from 189 GeV to 208 GeV. The  $q\bar{q}$  final states of the  $Z$  have been considered. The cross sections have been computed and compared with theoretical predictions.

Contributed Paper for EPS HEP 2001 (Budapest) and LP01 (Rome)

<sup>1</sup> CERN, Geneva, Switzerland

<sup>2</sup> On leave of absence from INFN Torino, Italy

# 1 Introduction

At LEP2 energies the radiative return to the Z boson is one of the dominant physics processes. Much less frequent is the process in which two high energy photons are emitted and a Z is produced at rest or with little boost.

This note studies the symmetric double radiative return events with a Z decaying into quarks. For  $Z \rightarrow q\bar{q}$  final states three different topologies have been analysed: when both photons are visible in the detector, when only one photon is visible and when both photons are lost in the beam pipe.

The efficiencies are estimated using the PYTHIA (version 6.125) simulation, and the cross sections are extracted as a function of the centre-of-mass energy.

## 2 Data and Monte Carlo simulation

During 1998 DELPHI recorded an integrated luminosity of  $158 \pm 1 \text{ pb}^{-1}$  at a mean energy of  $188.63 \pm 0.04 \text{ GeV}$ . During 1999 LEP delivered data at energies of  $191.6 \pm 0.1 \text{ GeV}$ ,  $195.5 \pm 0.1 \text{ GeV}$ ,  $199.5 \pm 0.1 \text{ GeV}$  and  $201.6 \pm 0.1 \text{ GeV}$ . DELPHI recorded an integrated luminosity of  $25.9 \pm 0.1 \text{ pb}^{-1}$ ,  $76.1 \pm 0.4 \text{ pb}^{-1}$ ,  $85.0 \pm 0.5 \text{ pb}^{-1}$  and  $41.8 \pm 0.2 \text{ pb}^{-1}$  at the four energies respectively. During 2000 LEP delivered data at the energies up to 208 GeV, concentrated around two mean values: 205 GeV and 206.5 GeV for an integrated luminosity of  $82.7 \text{ pb}^{-1}$  and  $141.7 \text{ pb}^{-1}$  respectively.

High statistics of background and signal events have been produced by Monte Carlo simulation using the DELPHI detector simulation program [1]. The signal events have been generated with PYTHIA [2] version 6.125 for  $e^+e^- \rightarrow q\bar{q}\gamma$ ,  $e^+e^- \rightarrow q\bar{q}\gamma\gamma$ , whereas KORALZ [3] for  $e^+e^- \rightarrow \mu\bar{\mu}\gamma$ ,  $e^+e^- \rightarrow \mu\bar{\mu}\gamma\gamma$ ,  $e^+e^- \rightarrow \tau\bar{\tau}\gamma$ ,  $e^+e^- \rightarrow \tau\bar{\tau}\gamma\gamma$ , PYTHIA and EXCALIBUR [4] were for the four-fermion background and TWOGAM [5] and BDK [6] for two-photon processes. BABAMC [7] was used to simulate Bhabha events.

## 3 Signal definition

A symmetric double radiative return event is an event where two photons of similar energies have been emitted (respectively by the  $e^+$  and the  $e^-$  lines) and a Z is produced almost at rest.

Ordering the photons according to their energy, and supposing them back to back, the following equation holds:

$$E_{\gamma_1} = \sqrt{s}/2 - M_Z^2/(2\sqrt{s} - 4E_{\gamma_2}) \quad (1)$$

and the second photon has maximal energy when:

$$E_{\gamma_2}^{max} = E_{\gamma_1} = (\sqrt{s} - M_Z)/2 \quad (2)$$

The energy of the photon in the single radiative return event is a limiting case of equation 1:

$$E_{\gamma}^{single} = (s - M_Z^2) / 2\sqrt{s} \approx 72 \text{ GeV} \text{ (at } \sqrt{s} = 189 \text{ GeV)} \quad (3)$$

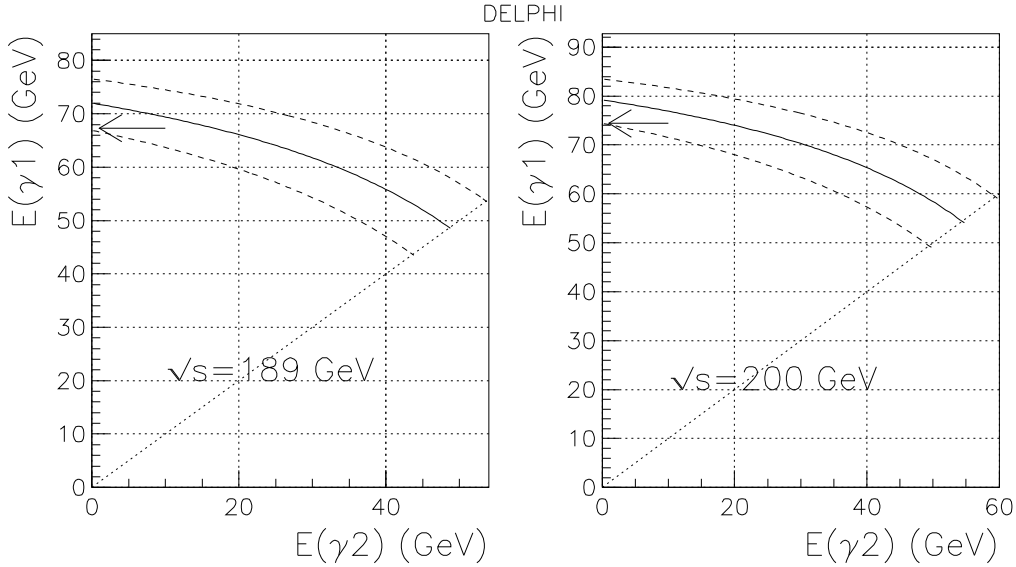


Figure 1: The full line is the relation between the two photon energies (described by equation 1), and the two dashed lines are obtained allowing a  $\pm 10$  GeV interval around the Z mass, at the two different centre-of-mass energies. The arrow defines the cut used to separate between the “single radiative return” from the “double radiative return” to the Z.

In the “single” radiative return event there can be emission of more than one photon but mostly in the same direction. That means that the sum of the energy of the 2 most energetic photons in the event in a single radiative return decay will be peaked at  $E = E_{\gamma}^{single}$  while for the symmetric double radiative decay the peak will occur at  $E = (\sqrt{s} - M_Z) \text{ GeV}$ .

In all these equations we neglected that the Z has a finite width. In practice the energy of the photons will be in a range expressing the width ( $\Gamma_Z$ ) of the Z boson. The final fermions are assumed to come from a Z boson decay if their invariant mass is within  $\pm 10$  GeV around the central value of 91.187 GeV. In figure 1 the energy of the first photon is shown (full line) as a function of the energy of the second photon. The two dashed lines represent a  $\pm 10$  GeV interval around the Z mass. The aim of this analysis is to study events where the Z is created with zero or small boost. To this extent the arrow shown in figure 1 separates the “single radiative return” from the “double radiative return” events.

The signal is defined by requiring that the most energetic photon of the event has energy lower than

$$E_{\gamma_1}^{max} = (s - (M_Z + 10)^2) / 2\sqrt{s} \quad (67 \text{ GeV at } \sqrt{s} = 189 \text{ GeV}). \quad (4)$$

and the second one has energy larger than  $E_{\gamma_2}^{min}$ , defined by equation 1 when  $E_{\gamma_1} = E_{\gamma_1}^{max}$ .

In figure 2.a the correlation between the sum of the two photon energies and the absolute difference of their polar angles ( $\theta$ ) is shown, when asking that the second photon

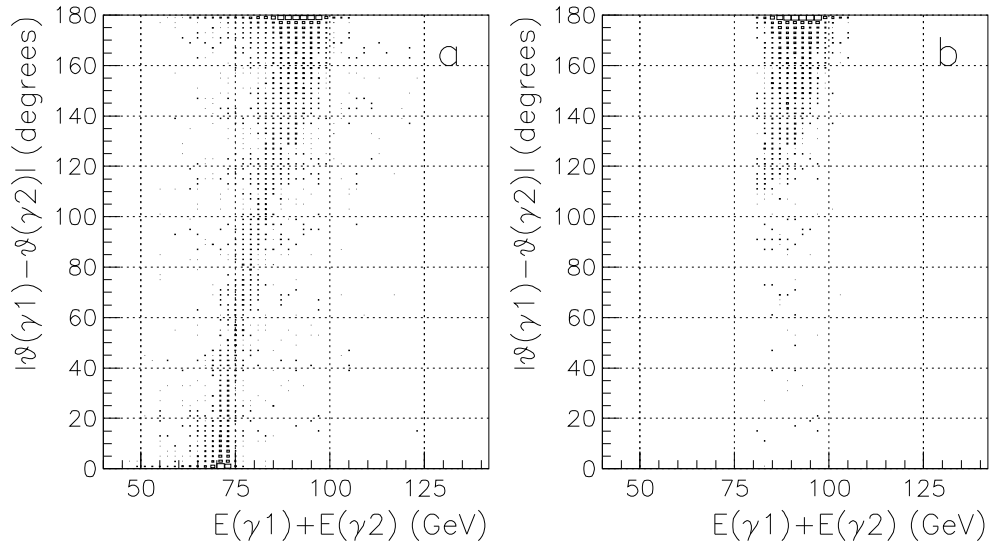


Figure 2: The distribution of the absolute difference of the two photon polar angles versus the sum of the two photon energies for simulated events at  $\sqrt{s}=189$  GeV. In a) asking  $E_{\gamma 2} \geq E_{\gamma 2}^{min}$  and in b) cutting also on the energy of the first photon as described in the text.

has energy larger than  $E_{\gamma_2}^{min}$  GeV (following equation 1) and in figure 2.b asking that the most energetic photon has energy lower than  $E_{\gamma_1}^{max}$ . The figure shows that the signal is mostly concentrated at values of the polar angle difference larger than  $90^\circ$ . So finally to select the signal it has been required that the difference between photon polar angles be greater than 90 degrees.

Figure 3.a shows the sum of the energy of the two most energetic photons from PYTHIA simulated events; one can see the peak of the radiative return events and, at higher energy, a smaller shoulder that is our signal. Asking that the second photon has energy larger than  $E_{\gamma_2}^{min}$ , the radiative return peak is considerably reduced as it is shown in figure 3.b, and finally in figure 3.c the relation between the two photon energy of equation 1 is applied, demanding  $E \leq E_{\gamma_1}^{max}$  and cutting on the difference of the photon polar angles. In fig. 3.c the dashed line reproduces fig. 3.a, showing how effective are the cuts based on kinematic constraints.

In figure 4(top) the Lorentz boost of the Z is shown as a full line for all the events, while the dashed line corresponds to the selected “double radiative return” events.

## 4 Analysis and results

### 4.1 Particle selection

Charged particles are selected if their momentum is greater than 100 MeV/c and if they originate from the interaction region (within 10 cm along the beam direction and within 4 cm in the transverse plane) and the error on the momentum estimation is less than 100%. Neutral particles are defined either as energy clusters in the calorimeters not associated to charged particle tracks, or as reconstructed vertices of photon conversions, interactions of neutral hadrons or decays of neutral particles in the tracking volume. All neutral clusters of energy greater than 100 MeV are accepted.

### 4.2 The photon identification

Electro-magnetic clusters are identified by a dedicated software program (REMCLU [8]) in all the three electro-magnetic calorimeters: HPC, FEMC, STIC. All the events with two identified photons (classified as tight or loose by REMCLU) are considered.

### 4.3 $Z \rightarrow q\bar{q}$ final state analysis

Sequential cuts are applied in order to reject the main background, keeping the signal efficiency as high as possible.

Events are selected if:

- the total number of charged tracks is more than 5;
- the total number of particles is more than 10.

The following cuts were applied to suppress the  $\gamma\gamma$  collisions and the Bhabha events:

- the total transverse momentum should be greater than  $0.16 \times E_{cm}$ ;

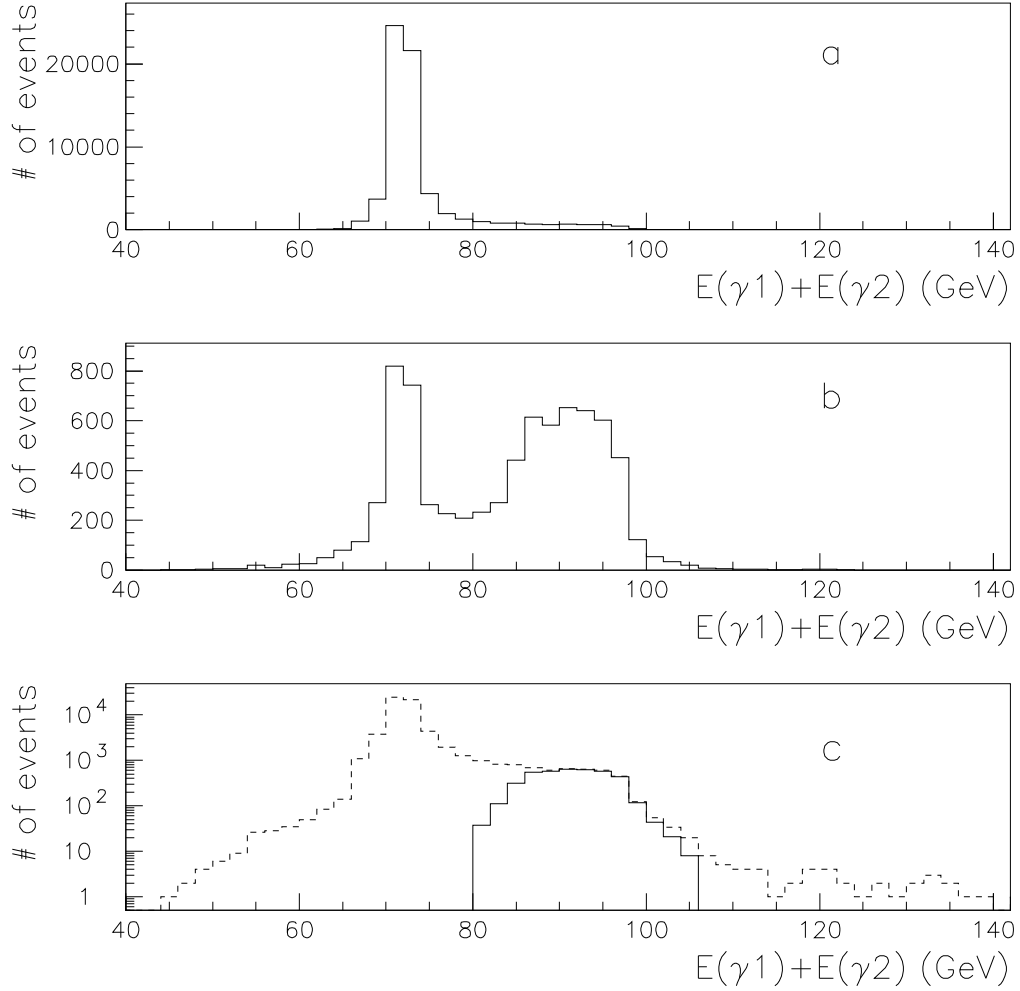


Figure 3: The sum of the energy of the two most energetic photons for simulated event with a Z at rest, at  $\sqrt{s}=189$  GeV. a) all the events; b) demanding the photons energy to be  $E \geq E_{\gamma_2}^{min}$ ; c) and applying the upper cuts on the energy of the photons and the cut on the difference of the two photon polar angle (full line). Superimposed in the last plot as a dashed line is the plot of figure a).

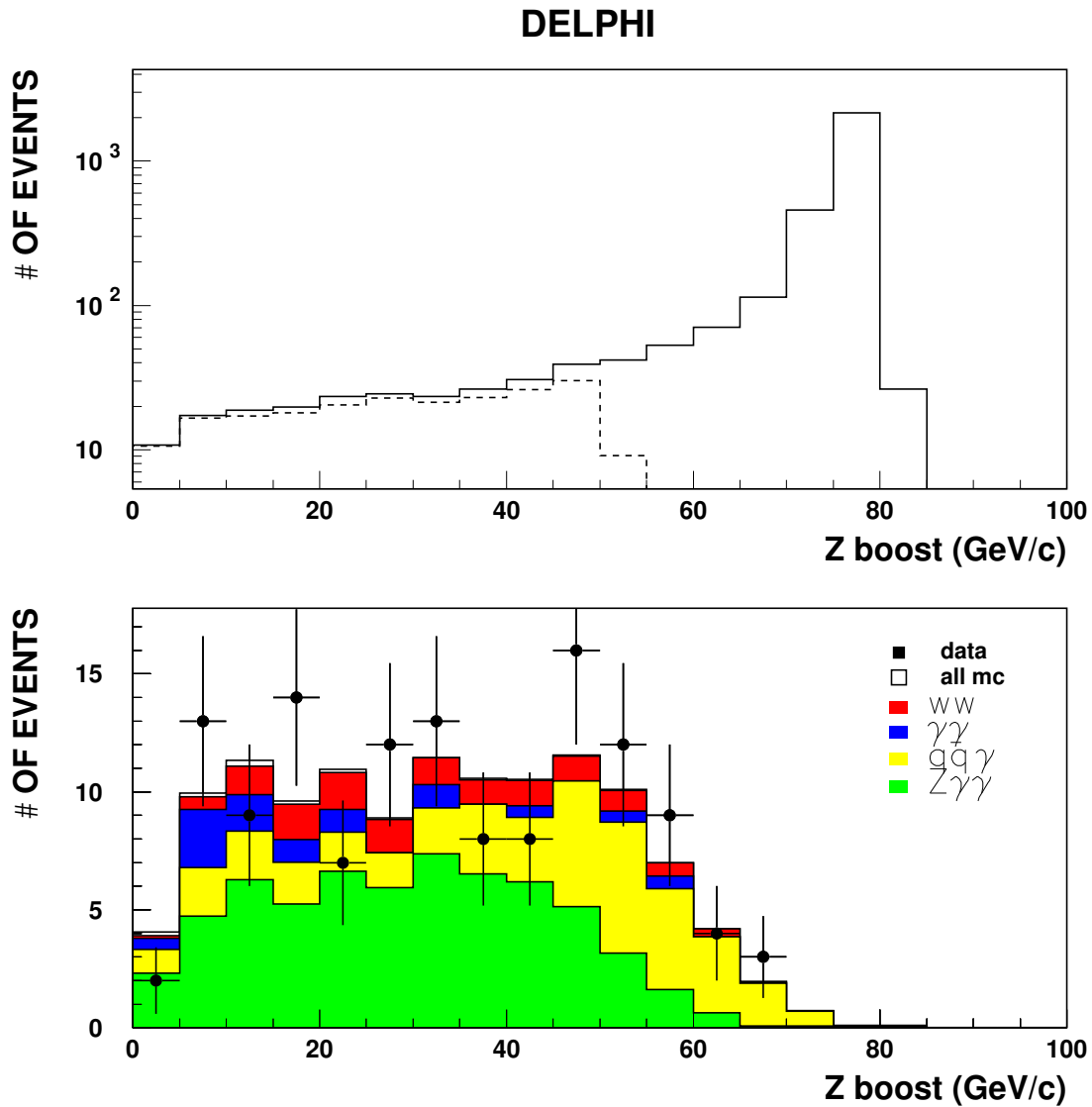


Figure 4: The upper plot shows the Lorentz boost of the Z for all the simulated  $q\bar{q}(\gamma)$  events (full line) and for the selected simulated “double radiative return events” (dashed line). The lower plot shows the Z Lorentz boost for data (points) and simulation (histograms) only for the events with the two photons lost in the beam-pipe. Both plots are for  $\sqrt{s}=189$  GeV

- the sum of the absolute value of the particles momenta along the thrust axis should be more than  $0.25 \times E_{cm}$ ;
- the electro-magnetic energy should be less than 80% of the total visible energy;
- no identified electron in the forward region (i.e.  $\theta \leq 40^\circ$ );
- no electro-magnetic clusters of energy higher than  $E_{\gamma 1}^{max}$

The total charged energy carried by VD-ID and VD only tracks is asked to be larger than 50% of the total charged energy in order to suppress off-momentum electrons and beam gas background.

After these cuts the difference in the total number of events in data and simulation is within a sigma at 192 GeV, 196 GeV, 202 GeV and 206.5 GeV, while the number of events in data is about 3 standard deviation above the simulation at the other energies, considering only statistical fluctuation.

### 4.3.1 Both photons in the detector

The percentage of events in which both photons are seen in the DELPHI detector, i.e.  $3^\circ \leq \theta \leq 177^\circ$ , is only 8% (estimated using the PYTHIA simulation).

In figure 5 the energy spectra of the two most energetic photons and the polar angle of the most energetic one are shown.

When the two photons have been identified, the cuts defined in section 3 to identify the signal are applied, and the remaining tracks are clusterized into 2 jets (using the Durham algorithm [9]). The angle between the photons and the nearest jet is required to be greater than 15 degrees. Next, energy and momentum conservation is imposed (keeping the direction of jets and photons fixed) to correct for bad energy and momentum reconstruction and finally the invariant mass of the 2 jets is computed. Table 1 displays the selected numbers of real and simulated events. Note that the signal events, defined in section 3, are a subsample of the PYTHIA  $q\bar{q}\gamma$  events. The top plot of figure 6 shows the invariant mass of the 2 jets for the selected events. All the energies are combined.

One of the selected events is shown in figure 7.

### 4.3.2 Only one visible photon

In the case where only one of the photons reaches the detector (36% of the cases) the kinematic can be constrained using the polar angle of the missing momentum. In this case the detected photon is requested to have energy between  $E_{\gamma 2}^{min}$  and  $E_{\gamma 1}^{max}$  and the difference between its polar angle and the polar angle of the missing momentum vector to be larger than  $100^\circ$ . The remaining tracks are clusterized into two jets and the angle between the photon and the nearest jet must be greater than 20 degrees. Energy and momentum conservation is imposed identifying the second lost photon with the missing momentum vector. To try to further reduce the background the following cuts are applied:

- total transverse momentum less than  $0.2 \times E_{cm}$ ;
- total momentum larger than  $0.1 \times E_{cm}$ ;
- total visible energy greater than  $0.45 \times E_{cm}$  and less than  $0.8 \times E_{cm}$ ;



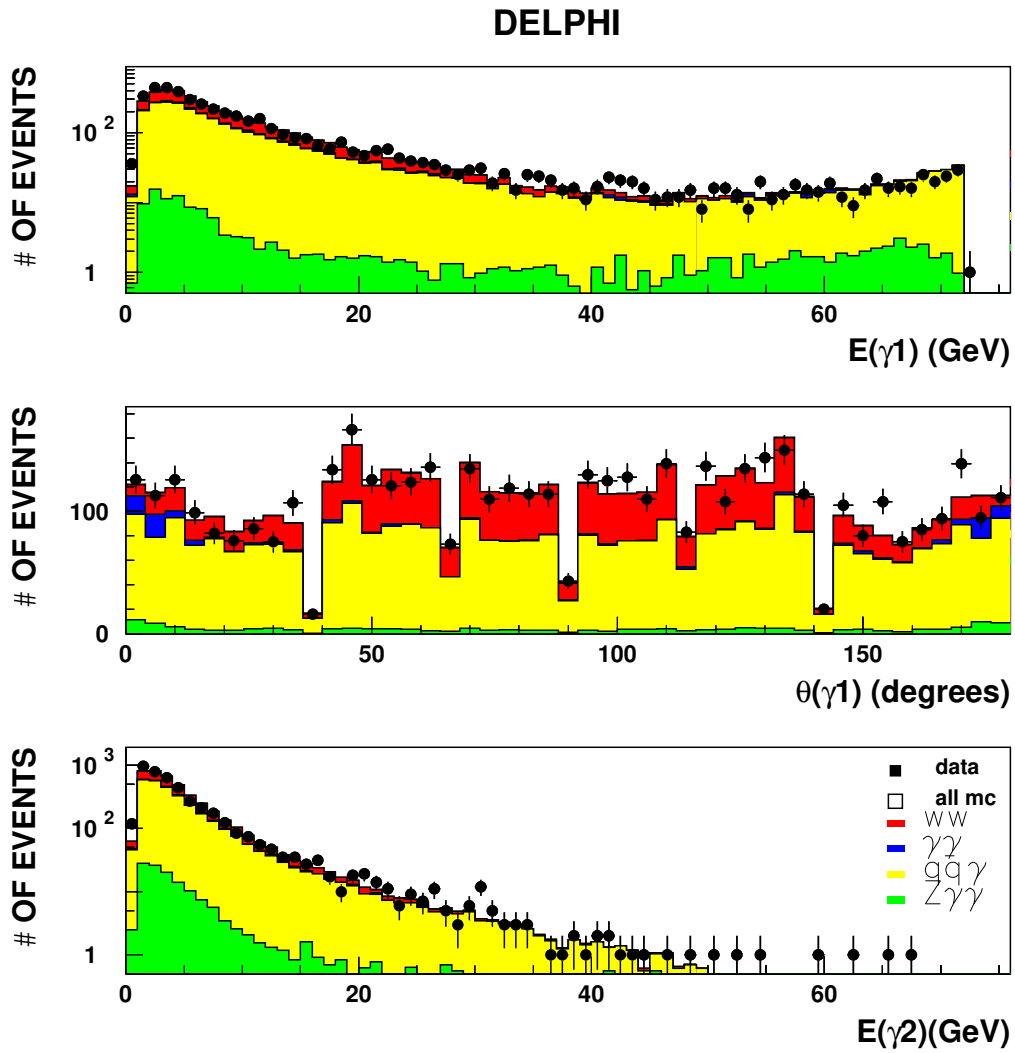


Figure 5: The distribution of the energy and of the polar angle of the most energetic photon, and, at the bottom, the energy of the second most energetic photon, at  $\sqrt{s}=196$  GeV.

- polar angle of missing momentum less than 30 degrees or greater than 150 degrees.

Table 2 displays the selected numbers of real and simulated events. Note that the signal events, defined in section 3, are a subsample of the PYTHIA  $q\bar{q}\gamma$  events. The middle plot of figure 6 shows the invariant mass of the 2 jets for the selected events and for all the energies combined together.

### 4.3.3 Non visible photons

The maximum of the cross section occurs when both photons get lost in the beam pipe. In this case only the 2 jets are detected and they are coplanar and collinear, with an invariant mass close to the  $Z$  mass and about 100 GeV missing energy.

The following, additional cuts are used to further suppress other sources of background:

- total missing momentum less than  $0.4 \times E_{cm}$ ;
- total transverse momentum less than  $0.15 \times E_{cm}$ ;
- the sum of the absolute value of the particles momenta along the thrust axis should be more than  $0.5 \times E_{cm}$ ;
- the electro-magnetic energy should be less than 70% of the total visible energy;
- total energy less than  $0.55 \times E_{cm}$  and greater than  $0.2 \times E_{cm}$ ;
- Events defined by this two-dimensional cut in the  $\theta(p_{mis})$  (degree) vs.  $\sqrt{s'}$  (GeV) plane are excluded:

$$\theta_{p_{mis}} < 90^\circ: \sqrt{s'} < (-0.39 \times \theta_{p_{mis}} + 115) \text{ GeV}$$

$$\theta_{p_{mis}} > 90^\circ: \sqrt{s'} < (+0.39 \times \theta_{p_{mis}} + 45) \text{ GeV}$$

- the maximum transverse momentum of a track with respect to a jet less than 10 GeV/c;
- energy of most energetic jet less than  $0.40 \times E_{cm}$ ;
- energy of less energetic jet less than  $0.25 \times E_{cm}$ ;
- charged multiplicity of jet greater than 1.
- acoplanarity between two jets less than 15 degrees;

Table 3 displays the selected numbers of real and simulated events. Note that the signal events, defined in section 3, are a subsample of the PYTHIA  $q\bar{q}\gamma$  events. Finally the invariant mass spectra for the selected events is shown in the bottom plot of figure 6 combining all the energies.

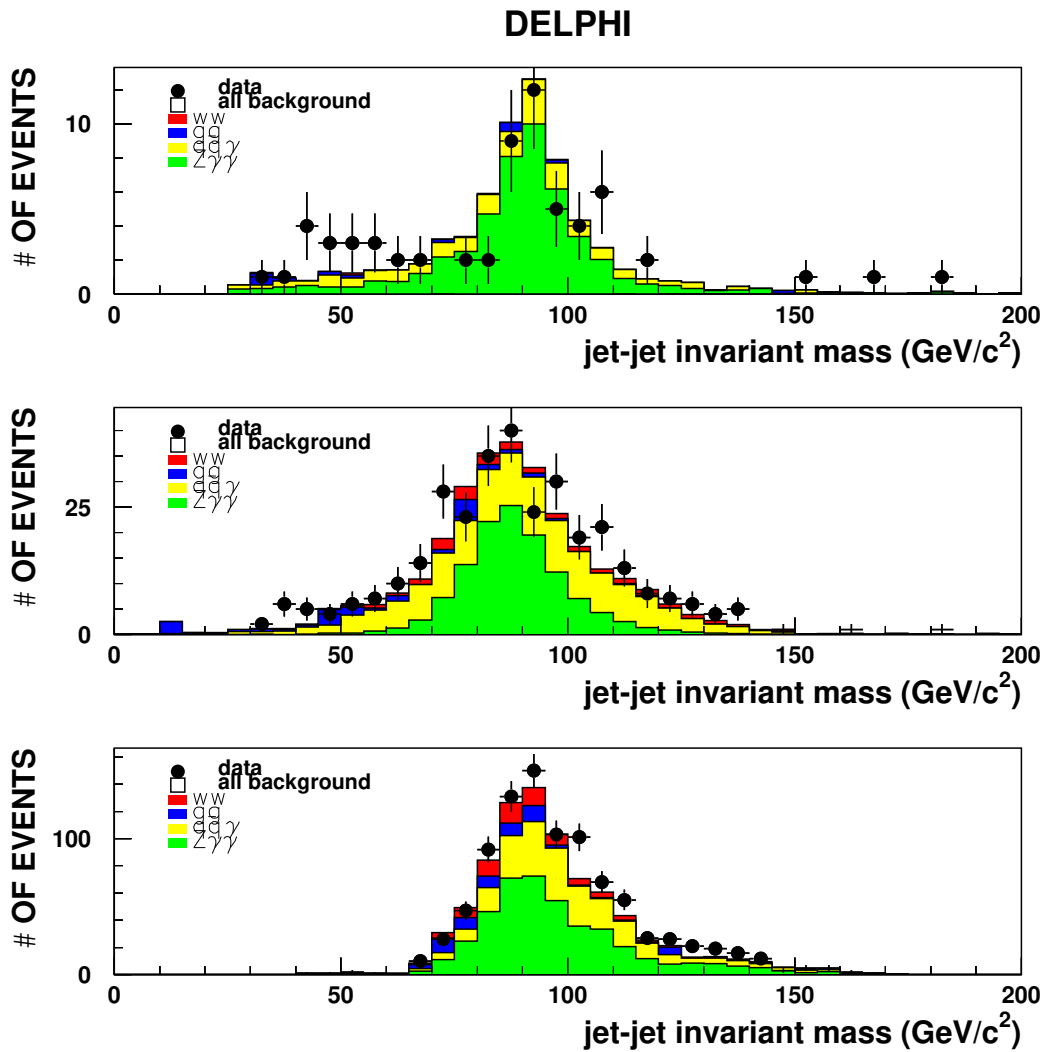



Figure 6: The two jets invariant mass combining all the energies ( $\sqrt{s}=189, 192, 196, 200, 202, 205$  and  $206.5$  GeV) for events with two (top), one (middle) or zero (bottom) visible photons.

	<b>DELPHI</b>	<b>Run :</b>	<b>88726</b>	<b>Evt :</b>	<b>85</b>													
	Beam:	94.6 GeV	Proc:	2-Dec-1998	Act	(	0	6	0	33	0	0	0					
	DAS:	6-Oct-1998	Scan:	23-Aug-1999	Deact	(	0	X235	X	0	X	33	X	0	X	0	X	0
		22:37:15		Tan+DST		(	0	0	0	0	0	0	0	0	0	0	0	

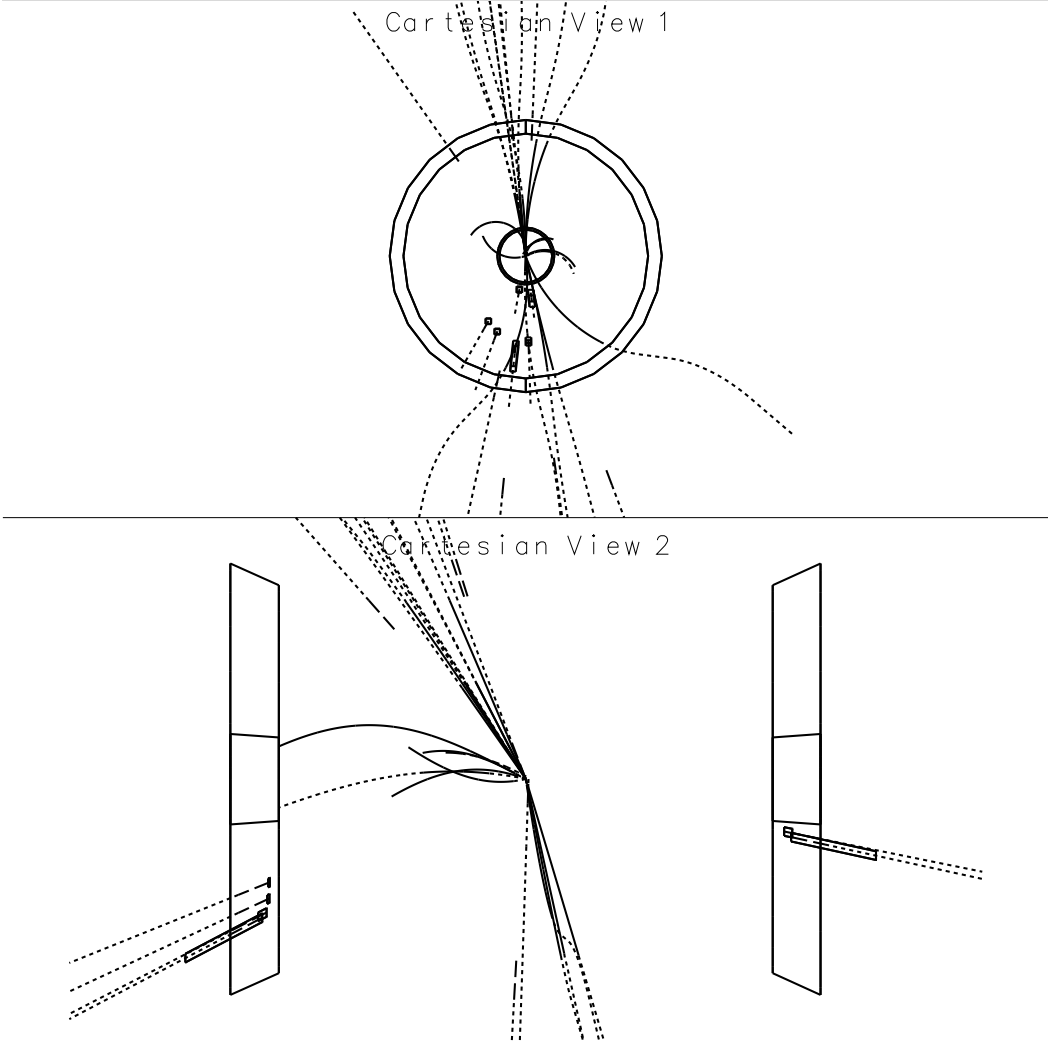


Figure 7: A selected event at  $\sqrt{s}=189$  GeV: top XY view, bottom XZ view (the electron and positron beams are along the Z axis). Two photons of 56.5 and 36.8 GeV are detected in the forward electro-magnetic calorimeter (FEMC) and the 2 jet invariant mass is 92.4 GeV/c<sup>2</sup>.

Energy	Data	MC	Signal
189 GeV	15	16.9	12.8
192 GeV	1	3.3	2.6
196 GeV	12	8.7	6.8
200 GeV	10	8.9	5.2
202 GeV	3	3.7	2.8
205 GeV	6	10.3	7.3
206.5 GeV	17	17.3	12.2

Table 1: Number of selected events in data and MC when both photons are visible in the detector.

Energy	Data	MC	Signal
189 GeV	92	85.2	42.9
192 GeV	13	13.8	6.2
196 GeV	40	37.6	17.4
200 GeV	43	34.5	12.3
202 GeV	17	17.0	7.3
205 GeV	41	37.5	13.7
206.5 GeV	74	63.1	23.0

Table 2: Number of selected events in data and MC when only one photon is visible in the detector.

Energy	Data	MC	Signal
189 GeV	254	228.3	118.5
192 GeV	49	41.0	21.4
196 GeV	123	116.8	59.9
200 GeV	133	111.2	50.9
202 GeV	62	51.6	27.2
205 GeV	109	103.3	57.0
206.5 GeV	195	173.6	95.5

Table 3: Number of selected events in data and MC when both photons are lost in the beam pipe.

Energy	2 $\gamma$ visible	1 $\gamma$ lost	2 $\gamma$ lost
	$3^\circ \leq \theta_\gamma \leq 177^\circ$		$\theta_\gamma \leq 3^\circ, \geq 177^\circ$
189 GeV	$0.37 \pm 0.03$	$0.25 \pm 0.01$	$0.35 \pm 0.01$
192 GeV	$0.47 \pm 0.14$	$0.36 \pm 0.08$	$0.48 \pm 0.06$
196 GeV	$0.40 \pm 0.06$	$0.26 \pm 0.03$	$0.38 \pm 0.02$
200 GeV	$0.38 \pm 0.06$	$0.24 \pm 0.03$	$0.34 \pm 0.02$
202 GeV	$0.36 \pm 0.06$	$0.23 \pm 0.03$	$0.32 \pm 0.02$
205 GeV	$0.55 \pm 0.09$	$0.28 \pm 0.05$	$0.33 \pm 0.02$
206.5 GeV	$0.55 \pm 0.09$	$0.28 \pm 0.05$	$0.33 \pm 0.02$

Table 4: Signal efficiency for the process  $Z\gamma\gamma$ ,  $Z \rightarrow q\bar{q}$ . The errors are statistical only.

Energy	2 $\gamma$ visible	1 $\gamma$ lost	2 $\gamma$ lost
	$3^\circ \leq \theta_\gamma \leq 177^\circ$		$\theta_\gamma \leq 3^\circ, \geq 177^\circ$
189 GeV	$0.19 \pm 0.06 \pm 0.02$	$1.27 \pm 0.23 \pm 0.07$	$2.68 \pm 0.29 \pm 0.09$
192 GeV	$0.03 \pm 0.08 \pm 0.08$	$0.59 \pm 0.38 \pm 0.13$	$2.39 \pm 0.56 \pm 0.28$
196 GeV	$0.33 \pm 0.11 \pm 0.05$	$1.02 \pm 0.32 \pm 0.10$	$2.32 \pm 0.38 \pm 0.11$
200 GeV	$0.20 \pm 0.09 \pm 0.03$	$1.03 \pm 0.32 \pm 0.12$	$2.56 \pm 0.40 \pm 0.13$
202 GeV	$0.14 \pm 0.12 \pm 0.03$	$0.81 \pm 0.44 \pm 0.12$	$2.92 \pm 0.60 \pm 0.16$
205 GeV	$0.07 \pm 0.05 \pm 0.01$	$0.76 \pm 0.28 \pm 0.13$	$2.38 \pm 0.39 \pm 0.15$
206.5 GeV	$0.16 \pm 0.05 \pm 0.03$	$0.87 \pm 0.22 \pm 0.15$	$2.58 \pm 0.30 \pm 0.16$

Table 5: Cross-section (in pb) for the process  $Z \gamma\gamma$ ,  $Z \rightarrow q\bar{q}$ . The first uncertainty is statistical, the second one systematic.

#### 4.4 $Z\gamma\gamma$ ( $Z \rightarrow q\bar{q}$ ) Cross Section

The efficiency to select the process is estimated using the PYTHIA Monte-Carlo and is provided in table 4 for all topologies and all energies. From the number of selected events (see tables 1,2,3) and the efficiencies, the cross sections are computed as a function of the centre-of-mass energy, for the hadronic decays of the Z boson.

The results are summarised in table 5 and in figure 8 (where the errors are statistical only).

The systematic error on these values has been estimated by varying the energy range of the accepted photon i.e. by varying the interval around the Z boson mass from  $\pm 10$  GeV to  $\pm 8$  GeV, by changing the value of  $E_{\gamma 2}^{min}$  by 2 GeV and by considering as photon only those identified as tight by REMCLU [8]. Finally the efficiency for each of the topologies was varied by the corresponding uncertainty.

Furthermore, if the discrepancy between data and simulation observed at the preselection level (see section 4.3), is entirely attributed to the accuracy of the  $q\bar{q}(\gamma)$  final state simulation, its effect (evaluated by a global rescaling of the  $q\bar{q}(\gamma)$  simulation) would translate into a 0.3 standard deviation decrease of the cross sections for 1 and 2 lost photons. This effect has not been considered for the moment in the final results, because further investigations are needed.

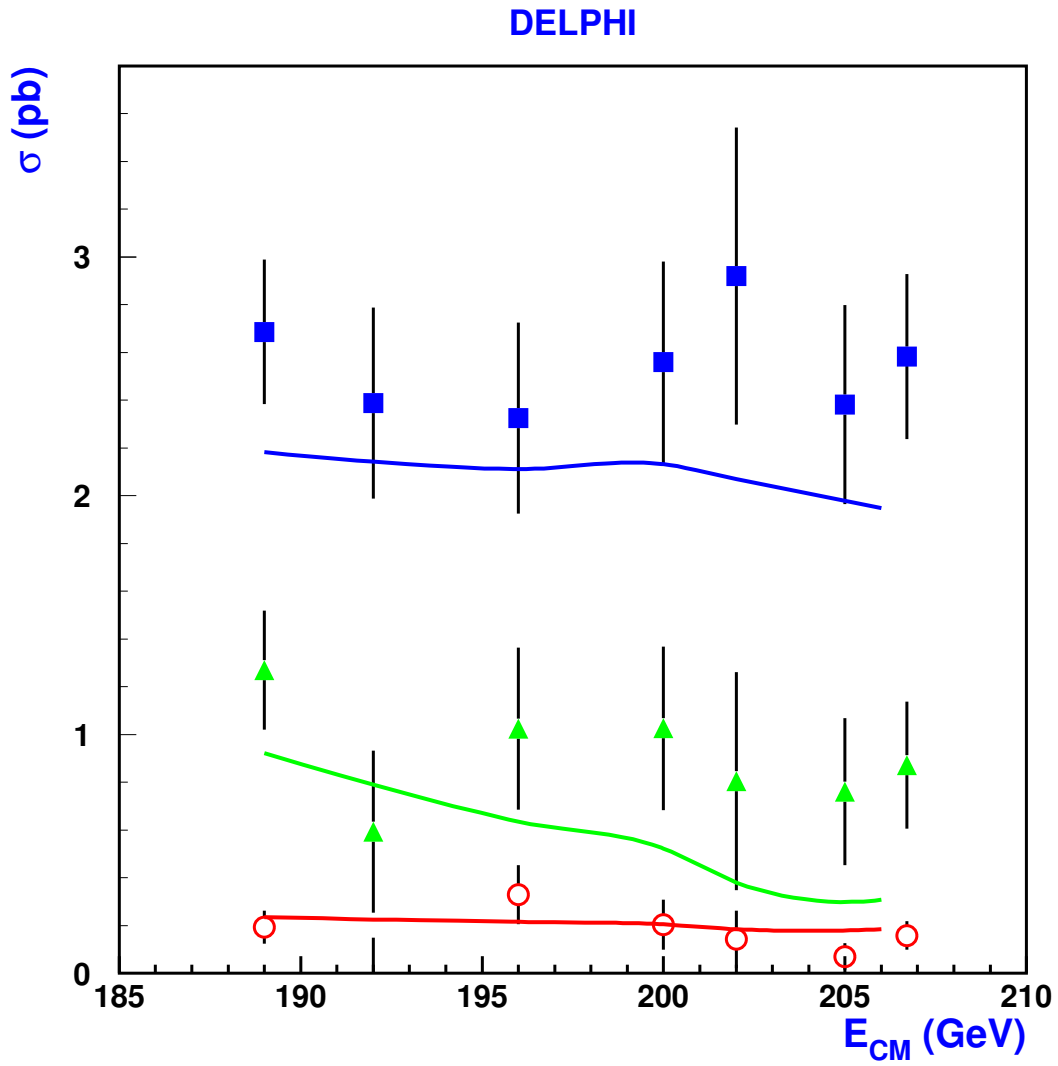


Figure 8: Cross sections at different centre-of-mass energy. The full lines represent the cross sections coming out from simulation based on PYTHIA 6.125 [2].

At the center of mass energies of 200 and 206.5 GeV the efficiencies and expected cross sections for the symmetric double radiative events have been estimated with the program KK2F (version 4.14) [11] and found in agreement within the statistical error.

## 5 Summary

The symmetric double radiative return has been studied at LEP. Preliminary measurement of the cross-section for this process has been performed at centre-of-mass energies of 189 GeV, 192 GeV, 196 GeV, 200 GeV, 202 GeV, 205 and 206.5 GeV and in three different experimental topologies: when both photons are detected, where one photon is lost in the beam-pipe and finally when both photons are lost. The measured cross section values range from about 2 pb when both photons are lost in the beam pipe, to fractions of a picobarn when both photons are visible in the detectors. The values observed in case of no visible photon and when only one photon is seen in the detector tend to always exceed by one to two standard deviation the the predictions of PYTHIA [2] and of KK2F [11]. This departure is under investigation, both for the purpose of the cross section determination and for the understanding of the irreducible QCD background in Higgs searches.

The L3 collaboration [12] performed recently a measurement of cross section for the process  $e^+e^- \rightarrow Z\gamma\gamma \rightarrow q\bar{q}\gamma\gamma$  within the following part of phase space: photon energies above 5 GeV, photons angles with respect to the beam axis between 14 and 166 degrees and invariant mass of the primary produced quark-pair before any radiation, within a  $\pm 2\Gamma_Z$  around the Z mass. Their result at the energies between 189 GeV and 202 GeV are compatible with the result shown in this paper.

## References

- [1] DELPHI Collaboration, P. Aarnio et al., Nucl. Instr. Meth. **303** (1991) 233.
- [2] T. Sjöstrand, Comp. Phys. Comm. **39** (1986) 347.
- [3] S. Jadach, B.F.L. Ward, Z. Was, Comp. Phys. Comm. **79** (1994) 503.
- [4] F.A. Berends, R. Pittau and R. Kleiss. Comp. Phys. Comm. **85** (1995) 437.
- [5] S. Nova, A. Olchevski and T. Todorov, in CERN Report 96-01, Vol. 2, p. 224 (1996).
- [6] F.A. Berends, P.H. Daverveldt and R. Kleiss, Nucl. Phys. **B253** (1985) 421; Comp. Phys. Comm. **40** (1986) 271, 285 and 309.
- [7] F.A. Berends, R. Kleiss, W. Hollik, Nucl. Phys. **B304** (1988) 712.
- [8] REMCLU, F.Cossutti, F.Mazzucato, A.Tonazzo, note in preparation.
- [9] S. Catani et al., Phys. Lett. **B269** (1991) 432; N. Brown, W.J. Stirling, Z. Phys. **C53** (1992) 629.
- [10] S. Andringa et al., 'ISR in hadronic events at LEP: generators versus data', DELPHI note 99-53 PHYS 824 PROG 237.



- [11] KK2F version 4.14, S.Jadach,B.F.L.Ward and Z. Was, Comp. Phys. Comm. 130 (2000) 260.
- [12] L3 Collab., M.Acciarri et al., CERN-EP/2001-008; January 26, 2001.